RAB-5 and RAB-10 cooperate to regulate neuropeptide release in *Caenorhabditis elegans*

Nikhil Sasidharan[a,b,c,1], Marija Sumakovic[a,c,1], Mandy Hannemann[a,d], Jan Hegermann[a,e], Jana F. Liewald[f], Christian Olendrowitz[a], Sabine Koenig[a,e], Barth D. Grant[g], Silvio O. Rizzoli[b,e], Alexander Gottschalk[f], and Stefan Eimer[a,e,h,2]

[a]Department of Molecular Neurogenetics, European Neuroscience Institute, 37077 Göttingen, Germany; [b]Stimulated Emission Depletion (STED) Microscopy of Synaptic Function, Department of Neuro- and Sensory Physiology, University of Göttingen, Göttingen, Germany; [c]International Max Planck Research School Neurosciences, 37077 Göttingen, Germany; [d]International Max Planck Research School Molecular Biology, 37077 Göttingen, Germany; [e]Department of Molecular Neurogenetics, Center for Molecular Physiology of the Brain, 37077 Göttingen, Germany; [f]Institute of Biochemistry, Johann Wolfgang Goethe University Frankfurt, 60438 Frankfurt, Germany; [g]Department of Molecular Biology and Biochemistry, Rutgers University, Piscataway, NJ 08854; and [h]Centre for Biological Signalling Studies (BIOSS), Albert-Ludwigs-University Freiburg, 79117 Freiburg, Germany

Edited by Iva Greenwald, Columbia University, New York, NY, and approved September 7, 2012 (received for review March 23, 2012)

Neurons secrete neuropeptides from dense core vesicles (DCVs) to modulate neuronal activity. Little is known about how neurons manage to differentially regulate the release of synaptic vesicles (SVs) and DCVs. To analyze this, we screened all *Caenorhabditis elegans* Rab GTPases and Tre2/Bub2/Cdc16 (TBC) domain containing GTPase-activating proteins (GAPs) for defects in DCV release from *C. elegans* motoneurons. *rab-5* and *rab-10* mutants show severe defects in DCV secretion, whereas SV exocytosis is unaffected. We identified TBC-2 and TBC-4 as putative GAPs for RAB-5 and RAB-10, respectively. Multiple Rabs and RabGAPs are typically organized in cascades that confer directionality to membrane-trafficking processes. We show here that the formation of release-competent DCVs requires a reciprocal exclusion cascade coupling RAB-5 and RAB-10, in which each of the two Rabs recruits the other's GAP molecule. This contributes to a separation of RAB-5 and RAB-10 domains at the Golgi–endosomal interface, which is lost when either of the two GAPs is inactivated. Taken together, our data suggest that RAB-5 and RAB-10 cooperate to locally exclude each other at an essential stage during DCV sorting.

neurosecretion | *trans*-Golgi | network | sorting

Fast synaptic transmission is mediated by the release of neurotransmitters from synaptic vesicles (SVs). In addition, neurons also release neuropeptides, hormones, and trophic factors from dense core vesicles (DCVs) to modulate neuronal activity and neurotransmission (1, 2). DCVs and SVs are anatomically and functionally distinct secretory organelles (3, 4). The mechanisms by which SVs and DCVs are differentially released by neurons are not clear.

In contrast to SVs, which can be recycled locally at the synapse, DCVs must be synthesized de novo in the cell body and replenished after exocytosis (5). DCV biogenesis starts at the *trans*-Golgi network (TGN), where neuropeptide precursors along with their processing enzymes, SNAREs, and vacuolar ATPases are packaged into DCVs. They bud off from the TGN as immature (i)DCVs, which subsequently undergo an extensive maturation process (5). During this maturation process, immature (i)DCVs are acidified. This activates furin-type proprotein convertases to proteolytically release active neuropeptides from their precursors. The active neuropeptides subsequently aggregate and form the dense core of DCVs. Mature (m)DCVs are formed after processing enzymes, SNAREs, required for homotypic iDCV fusion, and lysosomal proteins that have accidentally packaged into iDCVs are removed through sorting to the endosomal–lysosomal system (6). mDCVs competent for regulated secretion are then transported into the axon to the sites of release. DCVs and SVs require different conditions for exocytosis (7–9). However, despite their importance for the regulation of neuronal activity, very little is known about the molecular machinery, which differentially regulates DCV release.

Rab GTPases are master regulators of intracellular trafficking and have been shown to regulate SV release (10, 11). They are molecular switches that cycle between an active GTP-bound form and an inactive GDP-bound form. Through interactions with effector proteins, Rab GTPases control various steps of vesicular transport such as budding, tethering, and fusion (10). The activity state of Rab GTPases is regulated by auxiliary proteins called guanine nucleotide exchange factors (GEFs) and GTPase-activating proteins (GAPs), which facilitate their activation and inactivation, respectively (12). The human genome encodes over 60 Rab proteins (13). The actions of many of these Rabs have been shown to be organized in cascades. In a Rab-conversion cascade, a single Rab activates a secondary Rab by recruiting its respective GEF (14, 15). In contrast, during a Rab-exclusion cascade, a single Rab inactivates a secondary Rab by recruiting its respective GAP (16).

In a previous study, we showed that the Golgi-localized GTPase RAB-2 is a key regulator of neuronal DCV maturation in *Caenorhabditis elegans* (17, 18). We aimed here to identify additional Rabs that specifically regulate DCV biogenesis and secretion. By systematically testing all 22 Rab GTPases in *C. elegans*, we found that *rab-5* and *rab-10* mutants display severe defects in DCV but not SV release. This defect seems to occur because of a lack of reciprocal action of these Rabs on each other, through two specific GAP proteins, TBC-2 (RAB-5 GAP) and TBC-4 (RAB-10 GAP).

Results

rab-5 and _rab-10_ Mutants Display Severe Defects in DCV Secretion. DCV secretion from cholinergic motoneurons was assayed using a transgenic strain (*nuIs183*) expressing the proneuropeptide NLP-21 tagged to YFP (19) exclusively in dorsally projecting cholinergic motoneurons. This strain has been successfully used to assay DCV biogenesis and release (17–19). At the *trans*-Golgi, the proneuropeptide NLP-21-YFP fusion is packaged into DCVs, where it is subsequently processed into active neuropeptides and soluble YFP. YFP-labeled DCVs are then transported to axonal release sites. After fusion, the soluble YFP is released into the body cavity. Here, it is constitutively endocytosed by macrophage-like cells, called coelomocytes. The YFP fluorescence in coelomocytes can, therefore, be used as an indirect readout for DCV release (Fig. 1*A*). To identify Rabs that are regulating DCV release, we screened all viable *rab* mutants for defects in NLP-21-YFP secretion resulting in low coelomocytes fluorescence (Fig. 1*B* and Fig. S1). Rab GTPases, where the respective mutant was lethal or not available, were analyzed by RNAi or by neuronal expression of a constitutively active, GTP-bound mutant form (Fig. 1*B*). As a positive control, we used

Author contributions: N.S., M.S., M.H., B.D.G., S.O.R., A.G., and S.E. designed research; N.S., M.S., M.H., J.H., J.F.L., C.O., S.K., S.O.R., and A.G. performed research; N.S., M.S., M.H., J.H., and S.O.R. contributed new reagents/analytic tools; N.S., M.S., M.H., J.H., J.F.L., C.O., and S.O.R. analyzed data; and N.S., M.S., S.O.R., and S.E. wrote the paper.

The authors declare no conflict of interest.

This article is a PNAS Direct Submission.

[1]N.S. and M.S. contributed equally to this work.

[2]To whom corresponding should be addressed. E-mail: seimer@gwdg.de.

This article contains supporting information online at www.pnas.org/lookup/suppl/doi:10.1073/pnas.1203306109/-/DCSupplemental.

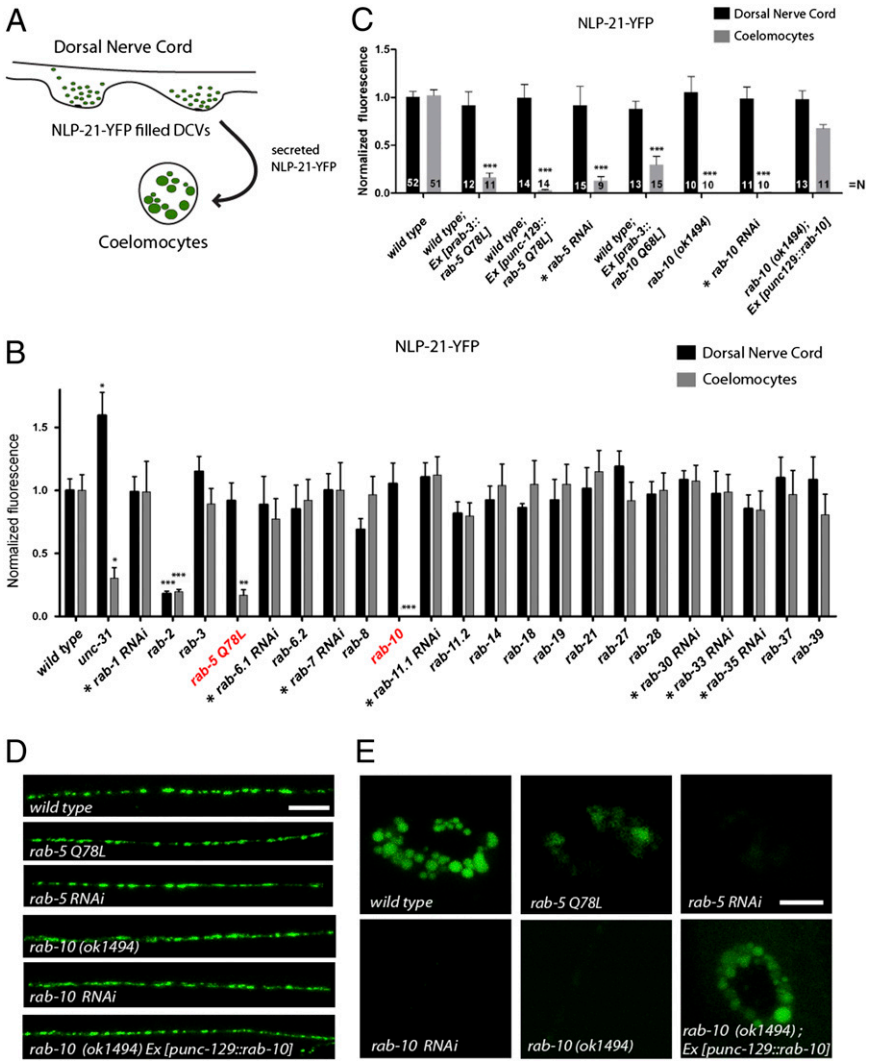

Fig. 1. RAB-5 and RAB-10 are regulators of DCV secretion. (*A*) Schematic describing the NLP-21-YFP assay used for analyzing DCV secretion in *C. elegans*. (*B*) All *rab* GTPase mutants were systematically tested for defects in NLP-21-YFP secretion. For Rabs where no mutant was available, tissue-specific knockdown was conducted in DA and DB cholinergic motoneurons (indicated by *) or a dominant-active variant was expressed and analyzed. Note: RNAi experiments were normalized to knockdown of mock vector (L4440). Error bars indicate SEM. $***P < 0.001$; $**P < 0.01$; $*P < 0.05$ (one-way ANOVA with Bonferroni post test). Representative pictures are shown in Fig. S1. (*C*) Secretion of NLP-21-YFP is impaired in *rab-5* and *rab-10* mutants Error bars indicate SEM. $***P < 0.001$; (one-way ANOVA with Bonferroni post test). (*D* and *E*) NLP-21-YFP fluorescence levels in the DNC are unaffected (*D*), whereas fluorescence levels in the coelomocytes are decreased (*E*). Tissue-specific knockdown of *rab-5* and *rab-10* in neurons showed similar defects in secretion. [Scale bars: 6 μm (in DNC); 4 μm (in coelomocytes).]

unc-31/CAPS mutants, which are known to have defects in DCV release (20). In this screen, we specifically identified RAB-5 and RAB-10 to be required for DCV secretion. DCV secretion was drastically reduced by around 83.24 ± 4.42% when a constitutively active, RAB-5 Q78L, mutant was expressed pan-neuronally or specifically in dorsally projecting cholinergic DA/DB motoneurons that also express the DCV marker NLP-21-YFP (Fig. 1 *B–E*). Similarly, expression of constitutively active RAB-10 Q68L also led to strongly impaired DCV secretion, whereas DCV release was completely abolished in the *rab-10 (ok1494)* deletion mutants (Fig. 1 *B–E*). This DCV secretion defect of *rab-5* and *rab-10* mutants was also confirmed using another DCV marker, the insulin-like neuropeptide INS-22-YFP (19) (Fig. S2).

Whereas the secreted DCV-derived YFP, as measured by the coelomocyte fluorescence, was dramatically decreased, the YFP intensity of dorsal axons appeared normal in *rab-5* and *rab-10* mutants. This suggests that the number of DCVs at release sites is unaffected in these mutants. This observation was confirmed by high-pressure freeze electron microscopic (HPF-EM) analysis, which showed normal DCV numbers at axonal release sites with a similar distribution and morphology compared with wild type (Fig. S3).

Because both secretion assays for NLP-21-YFP and INS-22-YFP are indirect assays, which rely on functional coelomocytes, it is conceivable that mutants affecting coelomocyte endocytosis would also display decreased coelomocyte YFP intensities. To demonstrate that coelomocyte function is unaffected in *rab-10* mutants or by neuronal expression of *rab-5 Q78L*, we analyzed the coelomocyte uptake of soluble Texas Red–conjugated BSA (TR-BSA) injected into the body cavity (21). Neither uptake nor the kinetics of endocytosis was affected in *rab-5 Q78L* and *rab-10* mutants (Fig. S4). This demonstrates that *rab-5* and *rab-10* mutant motoneurons display specific DCV-secretion defects.

To ensure that the observed DCV-secretion defects were cell-autonomous, we conducted tissue-specific knockdown of RAB-5 and RAB-10 by RNAi exclusively in the DA/DB cholinergic motoneurons and assessed for changes in NLP-21-YFP secretion (Fig. S5 *D–F*). In accordance with the mutant analysis, tissue-specific knockdown of *rab-5* and *rab-10* phenocopied the defect in NLP-21-YFP secretion with decreased YFP levels in coelomocytes (87.22 ± 4.76% and 99.99 ± 0.00%, respectively) (Fig. 1 *C–E*). Furthermore, transgenic lines expressing *mCherry-rab-10* exclusively in the DA/DB motoneurons rescued the DCV secretion defect in *rab-10* mutants (Fig. 1 *C–E*). These data suggest that RAB-5 and RAB-10 are required cell-autonomously in cholinergic motoneurons to regulate DCV release.

Synaptic Ultrastructure and SV Release Are Unaffected in *rab-5* and *rab-10* Mutants. RAB-5 and RAB-10 could be required for the release of SVs and DCVs. To exclude that RAB-5 and RAB-10 are required for SV release and synapse morphology, we initially analyzed two different SV markers, GFP-SNB-1 (synaptobrevin) and YFP-RAB-3. Both markers localize to SVs at synapses and can be viewed as discrete puncta in the dorsal nerve cord (DNC) axons when expressed in DA/DB cholinergic motoneurons. Each

NEUROSCIENCE

puncta highlights a neuromuscular synapse (22). Fluorescence intensities of puncta, puncta number, and puncta size of GFP-SNB-1 and YFP-RAB-3 were not different compared with wild type. These data suggest that SVs are localized correctly and that SV-containing synapses are largely unaffected (Fig. S3 *A* and *B*). To show that the synapse structures are not altered in *rab-5* and *rab-10* mutants, we analyzed presynaptic terminals using HPF-EM. Ultrastructural analysis of neuronal cell bodies, neuronal Golgi complexes, and synapses revealed no major alterations in their morphology (Fig. S3*C* and Fig. S6). In addition, the number and distribution of SVs at active zones of cholinergic motoneurons were also analyzed. No changes in SV numbers or in SV distributions were observed in *rab-5* and *rab-10* mutants (Fig. S3*D*).

To assess the integrity of SV release, all strains were tested electrophysiologically for changes in evoked postsynaptic currents (EPSCs). For this purpose, *rab-5* and *rab-10* mutants were crossed into a strain expressing channelrhodopsin-2 in the cholinergic motoneurons. Photo-evoked responses revealed no changes in EPSCs (Fig. S3*E*). All together, these data suggest that RAB-5 and RAB-10 are indeed factors specific for DCV release and not required for SV exocytosis.

RAB-10 Localizes to the Golgi–Endosomal Interface in Motoneurons. It has been shown that in the *C. elegans* intestine, RAB-5 localizes to the endo-lysosomal system (23, 24), and RAB-10 localizes to recycling endosomes (25). However, the precise localization of RAB-10 in *C. elegans* motor neurons remained unclear. Therefore, a detailed mapping of RAB-10 localization in *C. elegans* ventral nerve cord (VNC) neurons was conducted. Fluorescently labeled RAB-10 displayed partial overlap with markers for Golgi (Mannosidase II), endosomes (2xFYVE), and iDCVs (Syntaxin-6). No overlap was found with the ER marker cytochrome b_5 (CB5) or the early Golgi/Coat protein complex I (COPI) vesicle marker (εCOP) (Fig. 2*A*). In motoneuron axons mCherry-RAB-10 was largely diffuse and only partially colocalized with presynaptic markers, such as SV marker (YFP-RAB-3) and DCV marker (NLP-21-YFP) (Fig. 2*B*). DCVs are generally fewer in number at the active zone compared with SVs. Thus, it is likely that the partial localization of mCherry-RAB-10 at synaptic sites might suggest that RAB-10 is present on axonal DCVs. Interestingly, a recent proteomic analysis of DCVs enriched from vertebrate neurons also identified Rab10 (4). However, the strongest mCherry-RAB-10 signal was observed in motoneuron cell bodies where it partially colocalized with the DCV marker NLP-21-YFP (Fig. 2*C*), further suggesting that RAB-10 may be present on DCVs. We then analyzed the localization of RAB-10 relative to RAB-5. In cell bodies, mCherry-RAB-10 and YFP-RAB-5 only weakly overlapped and mostly localized to adjacent domains in close proximity (Fig. 2*D*; see also Fig. 5, below). These data suggest a function of RAB-5 and RAB-10 for DCV secretion at the Golgi–endosomal interface in cell bodies.

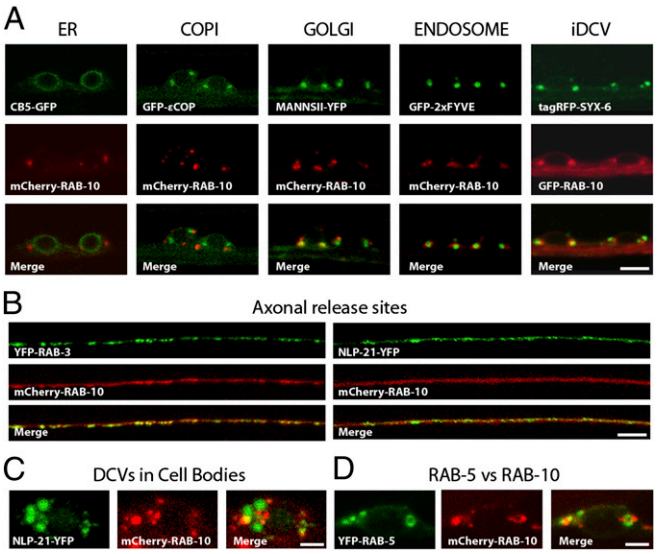

Fig. 2. Colocalization analysis of RAB-10. (*A*) Fine-mapping of the subcellular localization of RAB-10 in VNC neurons revealed no overlap with markers for the ER (CB5-GFP) and early Golgi/COPI vesicle (GFP-εCOP) and partial colocalization with markers for the medial Golgi (MannsII-YFP), endosomes (GFP-2xFYVE), and iDCVs (tagRFP-Syx-6). (Scale bar: 4 μm.) (*B*) RAB-10 is also enriched in axons at DNC synapses and showed colocalization with the SV marker (YFP-RAB-3) and DCV marker (NLP-21-YFP). (Scale bar: 5 μm.) (*C*) RAB-10 also displayed partial colocalization with the DCV marker (NLP-21-YFP) in neuronal cell bodies. (Scale bar: 1.5 μm.) (*D*) RAB-10 and RAB-5 localize to adjacent domains that rarely colocalize. (Scale bar: 1.5 μm.) Note: GFP-RAB-10 and tagRFP-SYX-6 are false-colored to enable simpler viewing.

Rab GAP Mutants *tbc-2* and *tbc-4* Display DCV Secretion Defects Similar to *rab-5* and *rab-10*. The function of Rab GTPases is regulated by GTPase-activating proteins (GAPs) and guanine nucleotide exchange factors (GEFs) (26). Whereas the Rab GEFs are very diverse on the sequence level, most Rab GAPs contain a clearly identifiable TBC (tre-2/cdc16/Bub2) domain. To identify possible RAB-5 and RAB-10 GAPs involved in DCV release, we systematically screened TBC domain–containing Rab GAP mutants for their involvement in regulating NLP-21-YFP secretion. The *C. elegans* Rab GAP mutants, *tbc-2* and *tbc-4*, displayed severe defects in DCV release similar to *rab-5* and *rab-10* mutants, respectively. Both an early-stop allele, *tbc-2 (qx20)*, and a deletion allele, *tbc-2 (tm2241)* (23), had reductions in coelomocyte YFP intensities by 71.36 ± 14.10% and 81.01 ± 4.00%, respectively, closely matching *rab-5 Q78L* mutants (83.24 ± 4.42%). Similarly, the coelomocyte YFP intensities were almost abolished in the two *tbc-4* deletion alleles, *tbc-4 (ok2928)* and *tbc-4 (tm3255)*, by 94.64 ± 2.10% and 95.82 ± 1.39%, respectively, phenocopying *rab-10* mutants (Fig. 3*A*). As in the case with *rab-10*, neuron-specific expression of *tbc-2* and *tbc-4* restored DCV secretion. In contrast, neuron-specific expression of catalytically inactive TBC domain mutants TBC-2 R689A and TBC-4 R155A were unable to rescue DCV-secretion defects in *tbc-2* and *tbc-4* mutants. This suggests that the GAP activity of TBC-2 and TBC-4 is essential for DCV secretion (Fig. 3*A*).

To exclude that *tbc-2* and *tbc-4* mutants affect synapse structure and synaptic vesicle release, we tested for defects in SV numbers, distribution, localization, and release by HPF-EM and electrophysiology. Analysis revealed that all measured properties of SVs were unaffected in *tbc-2* and *tbc-4* mutants (Fig. S3 *A–E*). These data suggest that the synaptic ultrastructure and SV release are unaltered in *tbc-2* and *tbc-4* mutants, similar to *rab-5* and *rab-10* mutants. It is likely that TBC-2 and TBC-4 regulate RAB-5 and RAB-10 activity, respectively, for DCV release in neurons.

TBC-4 Is a Putative GAP for RAB-10. Recently, TBC-2 has been indeed identified as a RAB-5–specific GAP (23). Therefore, given our data, it is likely that TBC-4 may be a RAB-10–specific GAP. TBC-4 contains an N-terminal TBC domain [106–316 aa; Simple Modular Architecture Research Tool (SMART) prediction] and three coiled coil (CC) domains at its C terminus (Fig. S7). To test whether TBC-4 binds to RAB-10, we used the yeast two-hybrid (Y2H) system, which has previously been used successfully to identify functional Rab-GAP pairs (27). The constitutively GTP-bound form of RAB-10 Q68L exclusively binds to the catalytically inactive TBC-4 R155A mutant but not to the catalytically active full-length TBC-4 (Fig. 3*C*). Furthermore, the constitutively inactive, GDP-bound form of RAB-10 T23N did not interact with TBC-4 R155A (Fig. 3*D*). An analysis of the localization of RAB-10 with respect to TBC-4 demonstrated that they colocalize in the cell body to discrete puncta near the Golgi (Fig. 3*F*). Therefore, it is likely that TBC-4 is indeed a GAP for RAB-10. In addition, TBC-4 is similar to the human TBC domain–containing oncogene Evi5 (28) and Evi5-like (Fig. S7), for which weak Rab10-GAP activity could be demonstrated (29).

Interestingly, GTP-bound forms of RAB-8 and RAB-11.1 were also found to interact with TBC-4, albeit with the CC domain located within the first 100 aa before the TBC domain (identified with SMART after alignment with TBC-4 orthologs) (Fig. 3*E* and Fig. S7).

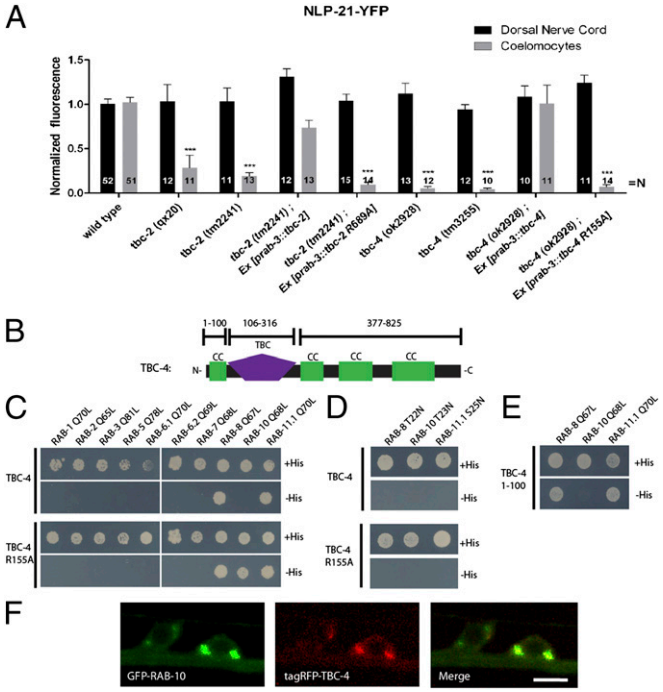

Fig. 3. Two Rab GAPs display impairments in DCV release similar to *rab-5* and *rab-10* mutants. (*A*) The Rab GAP mutants, *tbc-2* and *tbc-4*, have severe defects in DCV release. Error bars indicate SEM. ***$P < 0.001$ (one-way ANOVA with Bonferroni post test). (*B*) Schematic representation of the domain structure of TBC-4. CC, CC domain; TBC, tre-2/cdc16/Bub2 domain. (*C* and *D*) Full-length TBC-4 interacts with RAB-8 and RAB-11.1 (*C*) in a GTP-dependent manner (*D*). A catalytically inactive mutant of TBC-4 (R155A) specifically interacts with RAB-10 in a GTP-dependent manner. (*E*) RAB-8 and RAB-11.1 interact with an N-terminal CC domain of TBC-4 (1–100 aa). (*F*) TBC-4 and RAB-10 localize to the same compartments in VNC neurons. (Scale bar: 4 μm.)

This suggests that TBC-4 may also be an effector for RAB-8 and RAB-11.1, although it is unlikely that these interactions are required for DCV release, because depletion of *rab-8* or *rab-11.1* revealed no DCV-secretion defects (Fig. 1*B*). Moreover, RAB-8 and RAB-11.1 do not bind the TBC domain directly, so it is rather unlikely that TBC-4 might be a GAP for RAB-8 and RAB-11.1.

Two Effectors of RAB-5 and RAB-10 Phenocopy DCV-Release Defects. Activated Rab GTPases bind or recruit effector proteins, which then exert downstream functions (30). Therefore, we analyzed whether known RAB-5 and RAB-10 effectors are required for DCV secretion. Cell type–specific RNAi of the RAB-5 effector *rabn-5 (rabaptin-5)*, as well as the RAB-10 effector *ehbp-1* (31, 32), yielded no changes in NLP-21-YFP levels in the DNC axons but displayed a severe decrease in YFP fluorescence levels in the coelomocytes (*rabn-5*: 67.25 ± 14.80%; *ehbp-1*: 99.00 ± 0.20%), similar to *rab-5* and *rab-10* mutants, respectively (Fig. 4*A*). The observed phenotype was specific to these two effectors, because other known effectors such as early endosomal antigen-1 (EEA-1) did not reveal any DCV-release defects (Fig. 4*A*). These data suggest that there are two specific Rab-effector pairs required for DCV release. For directed membrane transport, Rab-effector complexes have been shown to be linked serially to form cascades. In such a cascade, a first Rab GTPase either activates or inactivates a second Rab by recruiting its GEF or GAP (15, 16). To determine whether a similar cascade existed between RAB-5 and RAB-10, we assayed possible interactions between TBC-2, RABN-5, TBC-4, and EHBP-1 by Y2H. We detected a specific interaction between the RAB-5 effector, RABN-5, and the presumptive RAB-10 GAP, TBC-4 (Fig. 4*B*). The RABN-5–binding domain of TBC-4 was confined to its C-terminal CC domain (TBC-4, 377–825 aa) (Fig. 4*B*). This interaction was also confirmed by coimmunoprecipitation in COS7 cells (Fig. 4*C*). In contrast, the N-terminal CC domains of RABN-5 (1–292 aa) bind to TBC-4 (Fig. 4*B*). This TBC-4–binding domain of RABN-5 is distinct from its RAB-5–interaction domain, which is located at the C terminus of RABN-5 (Fig. 4*B*). Because these binding domains are nonoverlapping, it is likely that activated, GTP-bound RAB-5 and TBC-4 can simultaneously interact with RABN-5. As expected from their direct interaction, TBC-4 and RABN-5 colocalized to discrete puncta in motoneuron cell bodies (Fig. 4*D*). Interestingly, further Y2H analysis showed that active, GTP-bound RAB-10 also interacts with the RAB-5 GAP, TBC-2 (Fig. 4*E*). Wild-type TBC-2 also interacted with RAB-8, RAB-18, and RAB-35. However, depletion of neither of these Rab GTPases showed defects in DCV secretion (Fig. 1*B*). It is, therefore, unlikely that these interactions are required for DCV release.

Reciprocal Exclusion of RAB-5 and RAB-10 by GAP Recruitment. Our results suggest that active RAB-5 would recruit the RAB-10 GAP, TBC-4, via Rabaptin-5 and that active RAB-10 would recruit the RAB-5 GAP, TBC-2. Thus, a domain of active RAB-5 would exclude RAB-10, whereas a RAB-10 domain would reciprocally exclude RAB-5 (Fig. 5*G*). This exclusion cascade would explain how two distinct Rab domains can be generated from a mixed precursor and then stably maintained in close proximity to each other (Fig. S8).

To directly test the reciprocal recruitment of the GAP in vivo, we expressed the dominant-active or -inactive variants of RAB-10 and RAB-5 and analyzed their ability to recruit TBC-2 and TBC-4, respectively (Fig. 5 *A* and *B*). As predicted by our Y2H data, active RAB-5 was localized to organelles where the RAB-10 GAP, TBC-4, was strongly recruited (Fig. 5 *B* and *C*). Conversely, active RAB-10 recruited TBC-2 (Fig. 5 *A* and *C*). The two GAPs were much more diffusely distributed when coexpressed with the dominant-inactive Rabs, confirming that their localization depends upon the activity of these Rabs (Fig. 5 *A*–*C*).

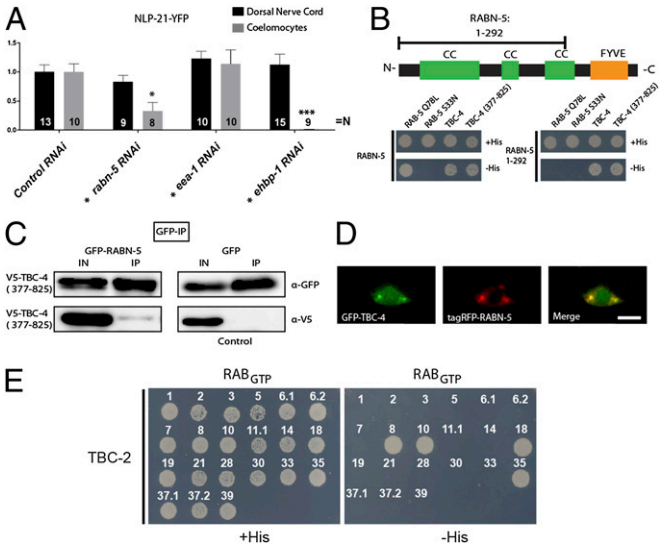

Fig. 4. Two Rab effectors also display impairments in DCV release. (*A*) Depletion of the RAB-5 and RAB-10 effectors, RABN-5 and EHBP-1, respectively, show defects in DCV release. Depletion of another RAB-5 effector, EEA-1, did not reveal any defect. Tissue-specific RNAi was conducted (as indicated by *). Error bars indicate SEM. ***$P < 0.001$; *$P < 0.05$ (one-way ANOVA with Bonferroni post test). (*B*) Schematic representation of the domain structure of RABN-5. Y2H analysis of RABN-5 and TBC-4 showed that the C-terminal CC domains of TBC-4 (377–825 aa) interacts with the N-terminal CC domains of RABN-5 (1–292 aa). CC, CC domains; FYVE, FYVE domain. (*C*) Coimmunoprecipitation of V5-TBC-4 (377–825 aa) and GFP-RABN-5 demonstrated that they also interact when expressed in COS7 cells. (*D*) TBC-4 and RABN-5 also localize to similar compartments in VNC neurons. (Scale bar: 4 μm.) (*E*) Y2H interaction analysis of full-length TBC-2 against *C. elegans* Rabs. TBC-2 interacts with GTP-bound RAB-8, RAB-10, RAB-18, and RAB-35.

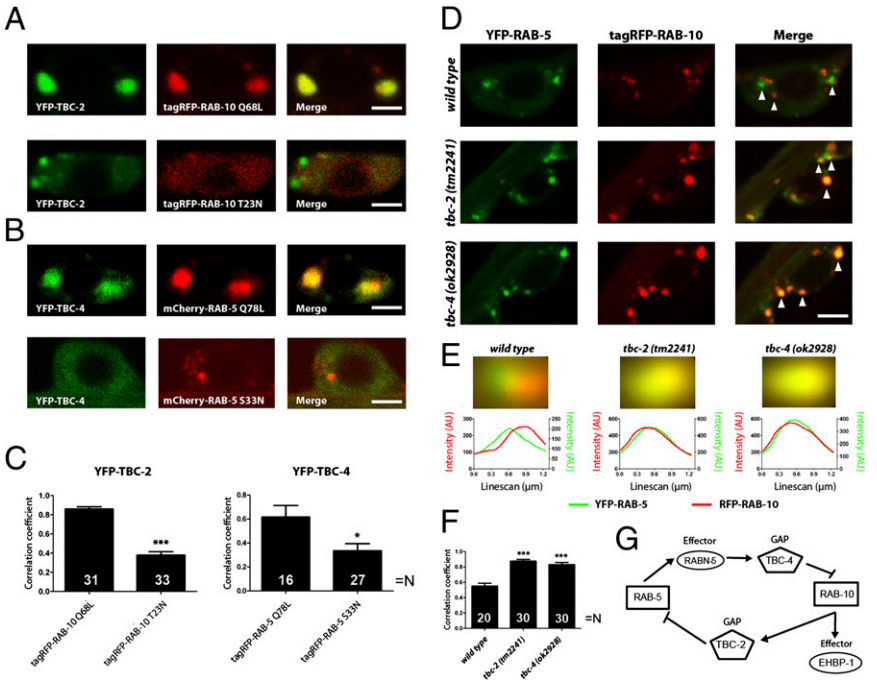

Fig. 5. GAP recruitment and domain formation by RAB-5 and RAB-10. (*A*) Typical images indicating the colocalization of dominant-active (Q68L) or -inactive (T23N) RAB-10 (fused to tagRFP, red), with the RAB-5 GAP, TBC-2 (fused to YFP, green). (*B*) Similar experiment performed for RAB-5 (fused to mCherry, red) and TBC-4 (fused to YFP, green). (Scale bar: 2 μm.) (*C*) Pearson's correlation coefficients were calculated for the different genotypes. Note that the active Rab variants correlate with each other's GAPs to significantly higher levels than inactive variants. ***$P < 0.001$; *$P < 0.05$ (Student's *t* test). (*D*) Colocalization between YFP-RAB-5 (green) and tagRFP-RAB-10 (red) in the presence or absence of the two GAPs. Arrowheads denote individual organelles. (Scale bar: 2.5 μm.) Note the increase in colocalization upon deletion of TBC-2 (middle images) or TBC-4 (bottom images). (*E*) The green and red images of YFP-RAB-5–containing organelles were averaged to determine organelle size and the distance between the positions of the RAB-5 and RAB-10 domains (see ref. 44 and *SI Materials and Methods* for details). The organelle colors indicate that the overlap is much higher in absence of TBC-2 or TBC-4. To obtain numeric information, we performed line scans in the two color channels (lower graphs). The separation between the peaks of the line scans indicates the distance between the green and red fluorescence signals (45); Gaussian fits to the individual scans indicate the organelle (domain) sizes. Note that whereas the two Rabs colocalize perfectly in the absence of TBC-2 or TBC-4, their signals are shifted by ~210 nm in the wild type (a value much lower than the organelle diameter, ~570 nm; 75–99 organelles were averaged for each genotype). (*F*) Pearson's correlation coefficients, calculated as above, give an additional indication that RAB-5 and RAB-10 colocalize better in the absence of TBC-2 or TBC-4. ***$P < 0.001$ (Student's *t* test). (*G*) Scheme describing the interplay between RAB-5 and RAB-10 (see *Discussion* for details).

To test whether the recruitment of the TBC-2 and TBC-4 GAPs set up exclusive nonoverlapping RAB-5 and RAB-10 domains, we compared the relative localization of RAB-5 and RAB-10 in wild-type and *tbc-2* or *tbc-4* mutant backgrounds. As expected by the exclusion model, we observed that YFP-RAB-5 and RFP-RAB-10 significantly colocalized in the absence of TBC-2 or TBC-4, whereas in wild-type neuronal cell bodies, both domains are segregated (Fig. 5 *D–F*). To determine whether this was attributable to the presence of RAB-5 and RAB-10 exclusively in different organelles in the wild type, or to the presence of separate domains on single organelles, we averaged the images of RAB-5–containing organelles for all three different genotypes (Fig. 5*E*). This procedure, when performed in absence of TBC-2 or TBC-4, provided an average organelle where the green (RAB-5) and red (RAB-10) signals correlated almost perfectly. However, in the wild-type background, the red and green signals were shifted by ~210 nm. Because this value is substantially below the average organelle diameter (~570 nm in this experiment), and because our imaging resolution is below the organelle size, this value indicates that separate Rab domains coexist on the same organelles.

Discussion

We have demonstrated that RAB-5 and RAB-10 are regulators of neuronal DCV release in *C. elegans*. Although almost all previous reports have placed RAB-5 and RAB-10 as a candidate required solely in the endocytic and recycling pathways (10, 15, 25 33), we propose that they have a function in controlling DCV secretion.

Previous studies have shown that PKC-1 selectively disrupts DCV release. Using a similar assay in *C. elegans*, it has been shown to reduce DCV secretion by about 50% (19). Interference with the RAB-5/RAB-10 cascade, however, reduces DCV release by 83% in the case of *rab-5* and literally abolishing release in the case of *rab-10*. Whereas impairment of UNC-13 affects DCV secretion, it also abolishes SV release (34, 35). UNC-31/CAPS has been suggested to only regulate DCV release in *C. elegans*. However, analysis of EPSCs in *unc-31* mutants demonstrated a decrease to about 50% of wild-type levels (20, 35). Initially, the decrease in SV release in *unc-31* mutants was suggested to be an indirect consequence of perturbed DCV secretion. Our data show that mutants with stronger DCV-release defects than *unc-31* have no effect on EPSCs. This supports the idea that in *C. elegans*, as in the mammalian system, UNC-31 may play a direct role in SV priming (19, 36). In addition, UNC-31 might also be required to regulate DCV numbers, because a deletion of *unc-31* in contrast to *rab-5/10* causes an accumulation of DCV in axons, which is enhanced in *unc-31; rab-10* double mutants (Fig. S2 *F* and *G*). This places RAB-5 and RAB-10, together with PKC-1, into a group of molecules fully dispensable for SV secretion and only required for DCV release.

Our results show that, in neurons, RAB-5 and RAB-10 primarily localize to puncta within the cell body. Based on their localizations, it is likely that these molecules are required at an early stage in the formation of mDCVs. We propose a model by which an iDCV membrane compartment acquires RAB-5– and RAB-10–positive domains that would enable an essential sorting step required for the formation of release-competent mDCVs. Active, GTP-bound RAB-5 molecules recruit their effector, Rabaptin-5/RABN-5, which has been implicated in early endosomal fusion (31). RABN-5 exists in a stable complex with Rabex-5/RABX-5 in mammalian cells and *C. elegans* (37, 38). Only as a complex is Rabaptin-5 efficiently recruited to endosomes. Thus, local activation of Rab5 would lead to the recruitment of this complex, which would further activate more Rab5 molecules in close proximity causing them to cluster (37). As demonstrated, this growing domain of active RAB-5 simultaneously eliminates RAB-10 by recruiting the RAB-10 GAP, TBC-4. Our results also showed that active, GTP-bound RAB-10 is able to bind and recruit the RAB-5 GAP, TBC-2, in vivo. Thus, these data also suggest a reciprocal elimination of RAB-5 from active RAB-10 domains. Such a RAB-5/RAB-10 exclusion mechanism would allow two defined membrane subdomains to form from a randomly ordered precursor compartment (Fig. 5*E* and Fig. S8). This mechanism would also allow these domains to be stably maintained on the same membrane patch in close proximity to each other, which is most likely a prerequisite for proper sorting between these domains.

Depletion of RAB-5 and RAB-10 does not affect DCV biogenesis, trafficking, and localization, as revealed by confocal microscopy and HPF-EM imaging (Figs. S2 and S3). However, the competence of DCVs to fuse is drastically reduced. A major

question still remains: what causes the inability of DCVs to be released in *rab-5* and *rab-10* mutants? The RAB-5/RAB-10 cascade could be required either to sort factors into DCVs for fusion or remove factors that are otherwise inhibitory to DCV release. Likely candidates for such molecules required for the initial steps of DCV biogenesis, which are later sorted away, are Syntaxin-6, vesicle-associated membrane protein (VAMP)4, and Synaptotagmin IV (5). Specifically in neurons and in neuroendocrine pituitary cells, the presence of Synaptotagmin IV on DCVs has been shown to inhibit DCV release (39–41). Thus, these molecules have to be sorted away for efficient release of DCVs.

Alternatively, the RAB-5/RAB-10 cascade could be required to sort specific molecules into DCVs that would be required for proper release. One possibility is that such molecules could be involved in remodeling filamentous (F)-actin at DCV-release sites. In bovine chromaffin cells, it has been shown that DCVs are prevented from accessing the exocytic sites by a barrier of cortical actin (42). After stimulation, several F-actin–serving pathways have been shown to be activated, facilitating recruitment of DCVs to the plasma membrane (42). These factors may be recruited directly by RAB-10, because we show that RAB-10 is also found at axonal release sites and perhaps even on DCVs (4, 43). After exclusion from the RAB-5 domain, RAB-10 could be subsequently recruited to a forming DCV domain. This membrane domain could be specified by the RAB-10 effector, EHBP-1, which is already membrane-localized independent of RAB-10 (32). Thus, EHBP-1 may recruit active RAB-10 to DCVs because elimination of either molecule prevents DCV release in a similar manner. How RAB-10 would be activated close to EHBP-1 is not yet clear. Interestingly, EHBP-1 possesses an actin-binding calponin-homology domain that may bind to actin. Therefore, it is tempting to consider that a reorganization of the actin network around DCVs may be a rate-limiting step for DCV release.

Since a wide range of biological processes are facilitated by DCVs, including neuronal development, blood glucose homeostasis, pain sensation, learning, and memory, a deeper knowledge of DCV-release mechanisms will, therefore, enable the development of specific therapeutic strategies to treat disorders caused by perturbed neuropeptide and insulin function such as diabetes.

Materials and Methods

Most experiments were performed according to previously published procedures and are explained in detail in *SI Materials and Methods*.

Strains and Genetics. All strains were cultured at 20 °C on OP50 *Escherichia coli*–seeded nematode growth medium (NGM) plates as described previously (44). All mutant and transgenic strains are described in *SI Materials and Methods*. Newly generated strains are listed in Tables S1 and S2.

ACKNOWLEDGMENTS. We thank Shohei Mitani (National Bioresource Project, Tokyo Women's Medical University School of Medicine) and the *C. elegans* Knockout Consortium for providing deletion strains used in this study. Some strains were provided by the Caenorhabditis Genetics Center (CGC), which is supported by the National Institutes of Health (NIH) National Center for Research Resources. This work was supported by a fellowship of the Göttingen Graduate School for Neurosciences and Molecular Biosciences (to N.S.), Deutsche Forschungsgemeinschaft (DFG) Grant GSC 226/1 (to N.S. and M.H.), Neuroscience Early Stage Research Training (NEUREST) fellowships from the European Union Sixth Framework Programme (to M.S.), and by DFG Grants GO1011/2-1 and EXC115/1 (Cluster of Excellence Frankfurt–Macromolecular Complexes) (to A.G.). B.D.G. was supported by NIH Grant GM067237. S.O.R. was supported by a Seventh Framework Programme grant from the European Research Council (ERC) (NANOMAP).

1. Hu Z, Pym EC, Babu K, Vashlishan Murray AB, Kaplan JM (2011) A neuropeptide-mediated stretch response links muscle contraction to changes in neurotransmitter release. *Neuron* 71:92–102.
2. Chalasani SH, et al. (2010) Neuropeptide feedback modifies odor-evoked dynamics in Caenorhabditis elegans olfactory neurons. *Nat Neurosci* 13:615–621.
3. Takamori S, et al. (2006) Molecular anatomy of a trafficking organelle. *Cell* 127:831–846.
4. Zhao B, et al. (2011) Transport of receptors, receptor signaling complexes and ion channels via neuropeptide-secretory vesicles. *Cell Res* 21:741–753.
5. Tooze SA, Martens GJ, Huttner WB (2001) Secretory granule biogenesis: Rafting to the SNARE. *Trends Cell Biol* 11:116–122.
6. Kim T, Gondre-Lewis MC, Arnaoutova I, Peng Loh Y (2006) *Dense-Core Secretory Granule Biogenesis* (Physiology, Bethesda).
7. Bruns D, Jahn R (1995) Real-time measurement of transmitter release from single synaptic vesicles. *Nature* 377:62–65.
8. Schneggenburger R, Neher E (2000) Intracellular calcium dependence of transmitter release rates at a fast central synapse. *Nature* 406:889–893.
9. Voets T (2000) Dissection of three Ca2+-dependent steps leading to secretion in chromaffin cells from mouse adrenal slices. *Neuron* 28:537–545.
10. Stenmark H (2009) Rab GTPases as coordinators of vesicle traffic. *Nat Rev Mol Cell Biol* 10:513–525.
11. Fukuda M (2008) Regulation of secretory vesicle traffic by Rab small GTPases. *Cell Mol Life Sci* 65:2801–2813.
12. Zerial M, McBride H (2001) Rab proteins as membrane organizers. *Nat Rev Mol Cell Biol* 2:107–117.
13. Pereira-Leal JB, Seabra MC (2001) Evolution of the Rab family of small GTP-binding proteins. *J Mol Biol* 313:889–901.
14. Mizuno-Yamasaki E, Medkova M, Coleman J, Novick P (2010) Phosphatidylinositol 4-phosphate controls both membrane recruitment and a regulatory switch of the Rab GEF Sec2p. *Dev Cell* 18:828–840.
15. Rink J, Ghigo E, Kalaidzidis Y, Zerial M (2005) Rab conversion as a mechanism of progression from early to late endosomes. *Cell* 122:735–749.
16. Rivera-Molina FE, Novick PJ (2009) A Rab GAP cascade defines the boundary between two Rab GTPases on the secretory pathway. *Proc Natl Acad Sci USA* 106:14408–14413.
17. Sumakovic M, et al. (2009) UNC-108/RAB-2 and its effector RIC-19 are involved in dense core vesicle maturation in Caenorhabditis elegans. *J Cell Biol* 186:897–914.
18. Edwards SL, et al. (2009) Impaired dense core vesicle maturation in Caenorhabditis elegans mutants lacking Rab2. *J Cell Biol* 186:881–895.
19. Sieburth D, Madison JM, Kaplan JM (2007) PKC-1 regulates secretion of neuropeptides. *Nat Neurosci* 10:49–57.
20. Speese S, et al. (2007) UNC-31 (CAPS) is required for dense-core vesicle but not synaptic vesicle exocytosis in Caenorhabditis elegans. *J Neurosci* 27:6150–6162.
21. Zhang Y, Grant B, Hirsh D (2001) RME-8, a conserved J-domain protein, is required for endocytosis in Caenorhabditis elegans. *Mol Biol Cell* 12:2011–2021.
22. Sieburth D, et al. (2005) Systematic analysis of genes required for synapse structure and function. *Nature* 436:510–517.
23. Chotard L, et al. (2010) TBC-2 regulates RAB-5/RAB-7-mediated endosomal trafficking in Caenorhabditis elegans. *Mol Biol Cell* 21:2285–2296.
24. Brown HM, Van Epps HA, Goncharov A, Grant BD, Jin Y (2009) The JIP3 scaffold protein UNC-16 regulates RAB-5 dependent membrane trafficking at C. elegans synapses. *Dev Neurobiol* 69:174–190.
25. Chen CC-H, et al. (2006) RAB-10 is required for endocytic recycling in the Caenorhabditis elegans intestine. *Mol Biol Cell* 17:1286–1297.
26. Hutagalung AH, Novick PJ (2011) Role of Rab GTPases in membrane traffic and cell physiology. *Physiol Rev* 91:119–149.
27. Haas AK, Fuchs E, Kopajtich R, Barr FA (2005) A GTPase-activating protein controls Rab5 function in endocytic trafficking. *Nat Cell Biol* 7:887–893.
28. Westlake CJ, et al. (2007) Identification of Rab11 as a small GTPase binding protein for the Evi5 oncogene. *Proc Natl Acad Sci USA* 104:1236–1241.
29. Itoh T, Satoh M, Kanno E, Fukuda M (2006) Screening for target Rabs of TBC (Tre-2/Bub2/Cdc16) domain-containing proteins based on their Rab-binding activity. *Genes Cells* 11:1023–1037.
30. Grosshans BL, Ortiz D, Novick P (2006) Rabs and their effectors: Achieving specificity in membrane traffic. *Proc Natl Acad Sci USA* 103:11821–11827.
31. Stenmark H, Vitale G, Ullrich O, Zerial M (1995) Rabaptin-5 is a direct effector of the small GTPase Rab5 in endocytic membrane fusion. *Cell* 83:423–432.
32. Shi A, et al. (2010) EHBP-1 functions with RAB-10 during endocytic recycling in Caenorhabditis elegans. *Mol Biol Cell* 21:2930–2943.
33. Gorvel JP, Chavrier P, Zerial M, Gruenberg J (1991) rab5 controls early endosome fusion in vitro. *Cell* 64:915–925.
34. Richmond JE, Davis WS, Jorgensen EM (1999) UNC-13 is required for synaptic vesicle fusion in C. elegans. *Nat Neurosci* 2:959–964.
35. Gracheva EO, et al. (2007) Tomosyn negatively regulates CAPS-dependent peptide release at Caenorhabditis elegans synapses. *J Neurosci* 27:10176–10184.
36. Jockusch WJ, et al. (2007) CAPS-1 and CAPS-2 are essential synaptic vesicle priming proteins. *Cell* 131:796–808.
37. Lippé R, Miaczynska M, Rybin V, Runge A, Zerial M (2001) Functional synergy between Rab5 effector Rabaptin-5 and exchange factor Rabex-5 when physically associated in a complex. *Mol Biol Cell* 12:2219–2228.
38. Sato M, et al. (2005) Caenorhabditis elegans RME-6 is a novel regulator of RAB-5 at the clathrin-coated pit. *Nat Cell Biol* 7:559–569.
39. Dean C, et al. (2009) Synaptotagmin-IV modulates synaptic function and long-term potentiation by regulating BDNF release. *Nat Neurosci* 12:767–776.
40. Zhang Z, Bhalla A, Dean C, Chapman ER, Jackson MB (2009) Synaptotagmin IV: A multifunctional regulator of peptidergic nerve terminals. *Nat Neurosci* 12:163–171.
41. Eaton BA, Haugwitz M, Lau D, Moore HP (2000) Biogenesis of regulated exocytotic carriers in neuroendocrine cells. *J Neurosci* 20:7334–7344.
42. de Wit H (2010) Morphological docking of secretory vesicles. *Histochem Cell Biol* 134:103–113.
43. Han D, et al. (2011) Detection of differential proteomes associated with the development of type 2 diabetes in the Zucker rat model using the iTRAQ technique. *J Proteome Res* 10:564–577.
44. Brenner S (1974) The genetics of Caenorhabditis elegans. *Genetics* 77:71–94.
45. Barysch SV, Jahn R, Rizzoli SO (2010) A fluorescence-based in vitro assay for investigating early endosome dynamics. *Nature Protocols* 5(6):1127–1137.